European Journal of Cancer (2012) **48**, 3414–3421

Available at www.sciencedirect.com

SciVerse ScienceDirect

journal homepage: www.ejcancer.info

The value of 3.0 Tesla diffusion-weighted MRI for pelvic nodal staging in patients with early stage cervical cancer

W.M. Klerkx [a,*], W.B. Veldhuis [b], A.M. Spijkerboer [c], M.A. van den Bosch [b], W.P. Mali [b], A.P. Heintz [a], S. Bipat [c], D.M. Sie-Go [d], J. van der Velden [e], H.W. Schreuder [a], J. Stoker [c], P.H. Peeters [f]

[a] *Department of Gynecology and Obstetrics, University Medical Center Utrecht, The Netherlands*
[b] *Department of Radiology, University Medical Center Utrecht, The Netherlands*
[c] *Department of Radiology, Amsterdam Medical Center, The Netherlands*
[d] *Department of Pathology, University Medical Center Utrecht, The Netherlands*
[e] *Department of Gynecology and Obstetrics, Amsterdam Medical Center, The Netherlands*
[f] *Julius Center for Health Sciences and Primary Care, Utrecht, The Netherlands*

Available online 24 July 2012

KEYWORDS
Cervix cancinoma
Lymph node metastasis
DWI
Diagnostic accuracy
Specificity

Abstract ***Objective:*** The purpose of this study is to investigate the diagnostic accuracy of 3.0 Tesla (3T) diffusion-weighted magnetic resonance imaging (MRI) in addition to conventional MRI for the detection of lymphadenopathy in patients with early stage cervical cancer compared to histopathological evaluation of the systematically removed pelvic lymph nodes as reference standard.
Methods: 68 fédération internationale de gynécologie obstétrique (FIGO) stage Ia2 to IIb cervical cancer patients were included. Sensitivity and specificity rates for two experienced observers were computed for the detection of lymphatic metastasis. Reproducibility of conventional MRI was tested by kappa statistics. The variables included in the analysis were: size of the long axis, short axis, ratio short to long axis and apparent diffusion coefficient (ADC).
Results: Nine patients had 15 positive pelvic nodes at histopathological examination. The sensitivity and specificity of lymphatic metastasis detection by predefined conventional MRI characteristics was 33% (95% Confidence Interval (CI) 3–64) and 83% (95% CI 74–93) on patient level, and 33% (95% CI 7–60) and 97% (95% CI 95–99) on regional level respectively for observer 1. For observer 2 the sensitivity was 33% (95% CI 3–64) and the specificity 93% (95% CI 87–100) on patient level, and 25% (95% CI 1–50) and 98% (95% CI 97–100) on regio-

* *Corresponding author:* Address: Department of Gynecology and Obstetrics, University Medical Center Utrecht, Heidelberglaan 100, 3584 CX Utrecht, The Netherlands. Tel.: +31 088 75556427; fax: +31 088 7555507.
E-mail address: w.klerkx@umcutrecht.nl (W.M. Klerkx).

http://dx.doi.org/10.1016/j.ejca.2012.06.022

nal level, respectively. The kappa-value for reproducibility of metastasis detection on regional level was 0.50. The short axis diameter showed the highest diagnostic accuracy (area under the curve (AUC) = 0.81 95% CI 0.70–0.91); ADC did not improve diagnostic accuracy (AUC = 0.83 95% CI 0.73–0.93).

Conclusions: Diffusion-weighted MRI did not result in additional diagnostic value compared to conventional MRI.

1. Introduction

Histopathological examination of lymph nodes is still regarded the gold standard for establishing lymph node involvement in early stage cervical cancer; treatment options depend on nodal status. The method to obtain this information is invasive and thus bears a risk of complications. Furthermore, due to early detection of tumours and the introduction of screening programs, the number of patients with positive lymph nodes is low: 85% turns out to be node-negative.[1] The consequence is that for these patients the justification of an invasive and expensive diagnostic method is debatable.

Lymph nodes can be evaluated by MRI using their size and morphological aspect as malignancy characteristics. The specificity of MRI to exclude lymph node metastasis in early stage cervical cancer patients is high (over 90%), facilitated by the fact that the prevalence of lymph node metastasis in this patient group is low.[1,2] The sensitivity on the other hand is limited due to the inability to detect lymphatic metastasis in normal-sized and -shaped nodes.[2,3] Diffusion-weighted MRI (DWI) has been suggested to improve the differentiation between normal and metastatic nodes by means of differences in signal intensity quantified as the apparent diffusion coefficient (ADC).[4,5] Preliminary studies showed promising results on nodal staging in cervical cancer patients.[6–8] However there is no consistent evidence on how to interpret ADCs, both positive and negative correlations were found between ADC and metastasis.[8,9]

We conducted a prospective cohort study in early stage cervical cancer patients about to undergo a systematic pelvic lymphadenectomy to investigate the diagnostic accuracy of fat-suppressed T2-weighted MRI scan and the added value of DWI at 3.0 T.

2. Patients and methods

2.1. Patients

Eligible patients were consecutive non-pregnant women with histopathologically confirmed cervical carcinoma and clinically staged as FIGO (International Federation of Gynaecology and Obstetrics) stage Ia2 to IIb. Women were over 18 years of age and scheduled for systematic pelvic lymphadenectomy. Patients were prospectively included in two tertiary referral clinics. Exclusion criteria were contra-indications for MRI, i.e. cardiac pacemaker, claustrophobia or surgical clips in the brain. The local ethics research committees approved the study and informed consent was obtained from all patients. The study was registered at http://clinicaltrials.gov at NCT00288821.

2.2. Conventional MR imaging

In both centres patients were scanned on a 3.0 T MR scanner using a phased-array sensitivity encoding (SENSE) torso or cardiac coil (Achieva, Philips Healthcare, Best, The Netherlands). The field of view was set from the pubic symphysis to the common iliac arteries. The scan parameters are shown in Table 1. The field of view was 360×360 mm for all conventional sequences, with a slice thickness of 4 mm and a 0 mm slice gap. This slice thickness and gap were chosen to compare DWI and conventional MRI slice by slice.

Table 1
Scan sequences.

	Axial T1 fast field echo	Axial T2 turbo spin echo	Axial fat-suppressed T2 SPAIR[a]	Sagittal fat-suppressed T2 SPAIR[a]	DWI[b]
Bandwidth (Hz)	1264.2				
Echo time (ms)	2.3	80	80	80	54
Repetition time (ms)	394	3429	2881	2881	5000
Flip angle (°)	75				
TSE (turbo spin echo)/ EPI factor		20			41
Inversion delay (ms)			110	110	

[a] Spectrally-selective adiabatic inversion recovery sequence.
[b] Spectral selection attenuated inversion recovery (SPAIR) fat-suppressed single shot spin-echo EPI (echo planar imaging) sequence.

The T2-SPAIR sequence used for lymph node evaluation was acquired with a matrix size of 512 × 512. The slice thickness and gap for the DWI sequence were 4 and 0 mm; the matrix was 256 × 256. Four *b*-values were used; 0, 150, 500 and 1000 s/mm^2.

2.3. Image analysis

2.3.1. Test phase

All images were assessed by two board certified oncological radiologists of which one (observer 1) was a fellowship-trained abdominal and oncological radiologist with 9 years of experience in gynaecologic imaging and 15 years in body imaging in general. Observer 2 was a fellowship-trained interventional radiologist with special interest in oncology with three years of experience. At start, a consensus meeting was organised during which aforementioned scan sequences of patients not included in the study were shown and evaluated to obtain standardised test evaluations. All analyses were done on a picture archiving and communications system (PACS) workstation (Philips EasyVision DX).

2.3.2. T2-weighted (T2W) image assessment

The observers had no knowledge of clinical characteristics or FIGO stage. All lymph nodes with a long axis diameter measuring more than 5 mm in axial direction were registered. The following characteristics were assessed: the axial sequence and slice at which the node was measured, the size (diameter of the long and short axis in millimetre), the border (spiculated, lobulated, indistinct or smooth) and the region (left and right external iliac, obturator fossa, common iliac). The position of a node was categorised in six anatomical regions: the external iliac region was defined as located medial and cranial to the external iliac vein, while the obturator region covered the caudal area of the external iliac vein until the internal iliac vessels. The common iliac region included lymph nodes from the bifurcation of the internal and external iliac arteries until the bifurcation of both common iliac arteries. These regions are similar to the surgical margins of the removed node bearing tissue. Based on conventional MRI sequences metastasis was predefined as: more than 10 mm in short axis diameter or more than 8 mm in long axis diameter with a rounded shape (defined as short:long axis ratio over 0.8). Each pelvic region was classified as either positive or negative based on the nodal assessment of the observers.

2.3.3. Additional DWI assessment

During the review process colour fusion images of the highest b-value diffusion-weighted data set and the anatomical T2-weighted data set were used to facilitate the detection of pelvic lymph nodes.[10] The ADC map was automatically processed with in-house developed software using four *b*-values, i.e. 0, 150,

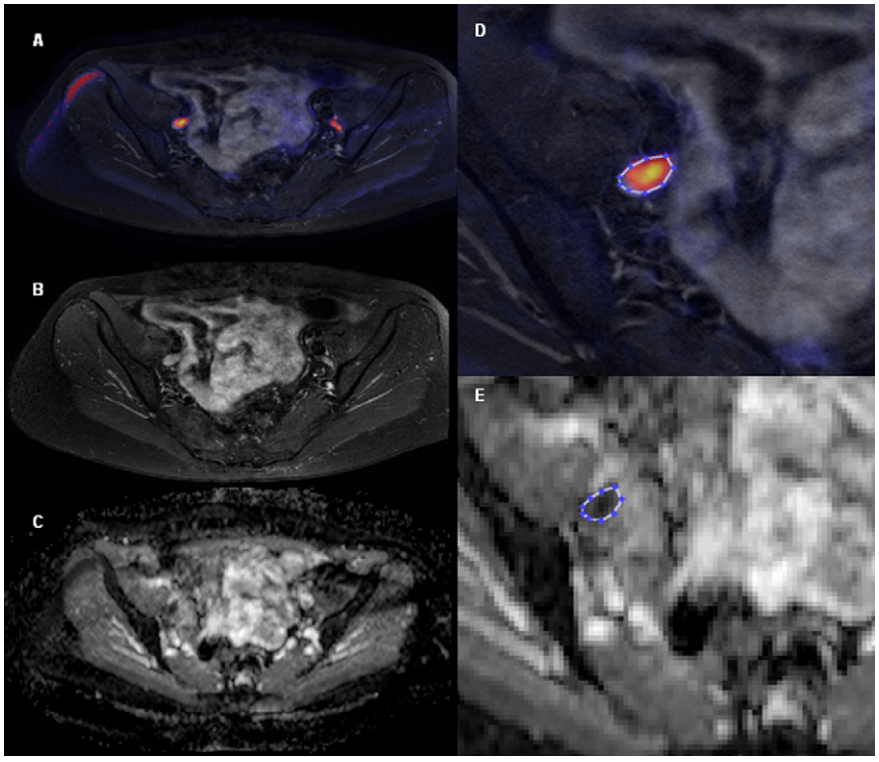

Fig. 1. A) Axial T2-weighted SPAIR, fused with DWI ($b = 1000$ s/m^2). Para-iliac lymph nodes are highlighted and easier to detect. (B) Axial T2-weighted SPAIR without the fusion image. (C) Apparent diffusion coefficient (ADC) map of this slice. (D) ADC measurement of the highlighted lymph node: a manually placed region of interest (ROI). (E) The ROI is then copied to the ADC map and manually adjusted if necessary.

500 and 1000 s/mm^2. A region of interest (ROI) was manually drawn by both observers on the transverse slice on which the maximal size of the lymph node was measured (Fig. 1). Small interspaces to the border were kept in order to prevent partial volume effect. The ROI drawn on the fusion image was automatically copied to the ADC map and manually adjusted if necessary. The mean ADC of a lymph node was used in the evaluation. For comparison of normalised ADCs, a ROI was drawn in the psoas muscle and, if it could be delineated, in the primary tumour.

2.4. Surgical procedure

Surgical procedures were performed by experienced gynaecological oncologists. A radical hysterectomy was combined with bilateral pelvic lymph node dissection (PLND) in all patients. The surgeons were blinded to the number and localisation of the pelvic lymph nodes detected by imaging. All lymph nodes were collected from the six anatomical regions. The primary tumour and lymphadenectomy specimens were sent to the pathologist separately for routine histopathologic examination.

2.5. Histopathology

After routine processing and embedding in paraffin of non-fixated lymph nodes, they were cut in parallel sections of 2 mm thickness. The sections were stained with Haematoxylin and Eosin and examined by a specialised pathologist in gynaecological oncology. The pathologist was blinded to the radiological findings. The pathologist counted the number of lymph nodes per anatomical site and scored the presence of metastasis per localised lymph node. Histopathological results were used as reference standard.

2.6. Image data versus histopathology

The lymph nodes detected by imaging were correlated to the surgical removed lymph nodes based on region and position by an independent reviewer. In some cases

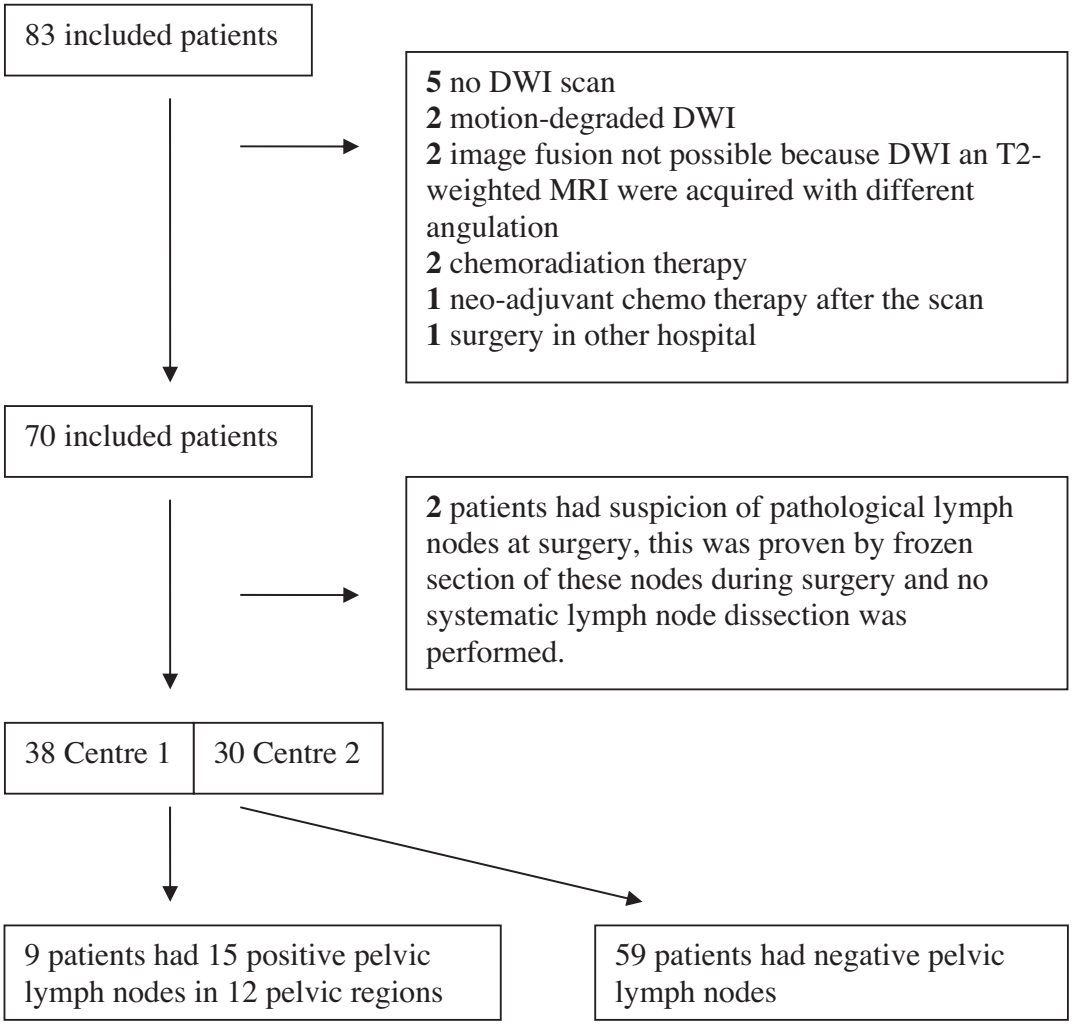

Fig. 2. Flowchart of included patients.

it was not possible to make a one-on-one correlation of the lymph nodes found at histopathological examination and those found by imaging. When the pathologist detected more lymph nodes than the radiologists observed by imaging, we chose the largest lymph node as the one most likely observed by imaging. For example, if the pathologist detected four lymph nodes in the right obturator region of which one was metastatic and three normal and the radiologists observed fewer nodes, the largest node measured by the observers was considered the malignant node.

2.7. Statistical analysis

To find an additional diagnostic value of 20% we computed (using $\alpha = 0.05$ and $\beta = 0.2$ and a sensitivity rate of 70% instead of 50% (with 95% confidence interval (CI) of ±25%)) 13 patients with pelvic lymph node metastasis would be needed.[2,3] With a pelvic lymph node metastasis rate of 15–20% approximately 74 patients should be included.

Frequency statistics were used for descriptive analysis. Normality was checked before proceeding with testing for differences between the observers (paired sample *t*-tests). If data were not normally distributed or categorical a Wilcoxon signed ranks test was used.

We computed sensitivity and specificity values with 95% CI per region and per patient for the predefined malignancy criteria, i.e. short axis >10 mm or long axis >8 mm and a round shape (short to long axis ratio >0.8). Kappa statistics were calculated to express interobserver agreement for classification of metastasized regions and patients. To test the added value of DWI, test performances with different threshold levels for all variables were computed and receiver operating characteristic (ROC) curves were estimated for the more experienced observer. The best performing variables were combined to compute optimal diagnostic accuracy. The new set of variables was tested with McNemar test for significant difference with the predefined malignancy criteria.

A *p*-value of less than 0.05 was considered statistically significant. Data were analysed using the Statistical Package for the Social Sciences version 15.0 (SPSS Inc., Chicago, IL). Sensitivity analyses were performed when patient characteristics were exceptional or could disturb test results.

3. Results

Eighty-three patients were included from February 2006 to 2009 (Fig. 2). After exclusion of 15 patients 68 patients could be included in the analysis. Nine of these patients had 15 positive lymph nodes in 12 pelvic regions (Table 2). Most patients (85.3%) had stage IbI disease, one patient had FIGO stage IIb and was included after neo-adjuvant chemotherapy. The mean duration between the scans and surgery was 19 days (range 1–44). Two patients had surgery more than 6 weeks after the scan.

Observer 1 detected more lymph nodes than observer 2 in all pelvic regions (Table 3). However, still only 25.5% of nodes histologically confirmed were detected by this observer. Almost all histologically confirmed malignant nodes were detected by both radiologists (100% for observer 1, 80% for observer 2). However the majority of these detected lymph nodes were not classified as such by the predefined malignancy criteria (i.e. short axis >10 mm or long axis >8 mm and a round shape (short to long axis ratio >0.8): 4 out of 15 lymph nodes for observer 1 and 3 out of 15 lymph nodes for observer 2. The remaining metastatic lymph nodes were too small or too elongated to be characterised as metastasis. On regional level the sensitivity of lymphatic metastasis detection was 33.3% (95% CI 6.7–60.0) with a specificity of 96.7% (95% CI 94.9–98.5) for observer 1 and 25.0% (95% CI 0.5–49.5) and 98.2% (95% CI 96.9–99.5), respectively for observer 2. The interobserver agreement was 0.50 on regional level and 0.42 on patient level.

When analysing the difference in malignancy characteristics between normal and metastatic nodes the following results were seen: short and long axis diameters are both significantly larger in metastatic nodes

Table 2
Tumour characteristics of 68 patients.

	Number (mean ± SD)	% (range)
Stage of disease		
Ia2	2	2.9
Ib1	58	85.3
Ib2	4	5.9
IIa	3	4.4
IIb	1	1.5
Age at inclusion (years)	44.3 (±10.1)	22.4–75.4
Days between scan and surgery	19.3 (±10.5)	1–44
Symptoms at time of diagnosis		
None, routine cytology	26	38.2
Postcoital bleeding	23	33.8
Abnormal uterine bleeding	18	26.5
Abdominal pain	1	1.5
Type of carcinoma		
Squamous cell carcinoma	47	69.1
Adenocarcinoma	16	23.5
Adenosquamous cell carcinoma	4	5.9
Clear cell carcinoma	1	1.5
Differentiation grade of tumour		
Good	5	7.4
Moderate	33	48.5
Poor	10	14.7
Missing	20	29.4
Smoking		
Never	31	45.6
Quit	11	16.2
Actual	25	36.7
Missing	1	1.5

Table 3
Characteristics of conventional MRI, diffusion weighted MRI and histology.

	Observer 1 *N* (% of histopathological counted nodes)	Observer 2 *N* (% of histopathological counted nodes)	Histology
Number of nodes			
Obturator region	280 (35.3%)	95 (12.0%)	793 (100%)
External iliac region	97 (13.7%)	116 (16.4%)	707 (100%)
Common iliac region	78 (40.6%)	22 (11.5%)	192 (100%)
Total	455 (25.5%)	233 (13.0%)	1786[a] (100%)
Metastasis	18 lymph nodes in 17 regions in 13 patients (1–3 per patient)	10 lymph nodes in 10 regions in 7 patients (1–2 per patient)	15 lymph nodes in 12 regions in 9 patients (1–3 per patient)
	Median (interquartile range) **Mean** (±SD)	**Median** (interquartile range) **Mean** (±SD)	***p***
Short axis diameter(mm)	4.8 (4.0–5.9)	5.0 (4.0–5.9)	0.00[b]
Long axis diameter(mm)	9.7 (7.3–12.4)	11.0 (8.6–13.7)	0.79[b]
Ratio short:long axis	0.54 (0.40–0.69)	0.47 (0.34–0.64)	0.00[b]
Border			
Smooth	327 (71.9%)	188 (80.7%)	
Spiculated	7 (1.5%)	0 (0%)	
Lobulated	112 (24.6%)	26 (11.2%)	
Indistinct	9 (2.0%)	19 (8.2%)	

[a] In three patients the number of lymph nodes detected at histopathological examination was not recorded per anatomic region.
[b] Wilcoxon signed ranks test.

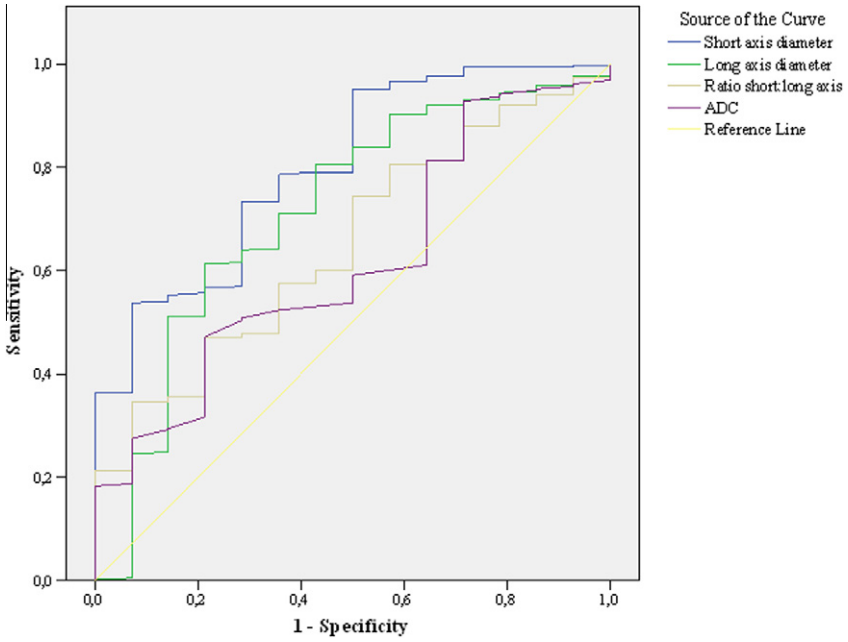

Fig. 3. Receiver operating characteristic (ROC) curves of morphological characteristics on conventional MRI. AUC short axis diameter with 95% Confidence Interval (CI): 0.81 (0.70–0.91). AUC long axis diameter with 95% CI: 0.69 (0.54–0.84). AUC ratio short:long axis diameter with 95% CI: 0.67 (0.54–0.79). AUC apparent diffusion coefficient (ADC) with 95% CI: 0.62 (0.48–0.76).

(5.1 mm versus 8.2 mm, $p = 0.00$ and 10.2 mm versus 12.6 mm, $p = 0.04$ respectively for observer 1 and 5.2 mm versus 7.9 mm, $p = 0.00$ and 11.1 mm versus 14.3 mm, $p = 0.03$ for observer 2). The ADC was not significantly different in metastatic nodes (0.62×10^{-3} versus 0.67×10^{-3} mm^2/s, $p = 0.06$ for observer 1 and 0.64×10^{-3} versus 0.72×10^{-3} mm^2/s, $p = 0.06$ for observer 2 respectively).

The criterion 'short axis diameter' had the best AUC (0.81 95% CI 0.70–0.91, Fig. 3). Adding ADC as variable only slightly improved the AUC (0.83 95% CI 0.73–0.93). The sensitivity and specificity of short axis

Table 4
Diagnostic accuracy at different cut-off values for all malignancy criteria per pelvic region.

Characteristic	AUC (95% Confidence Interval (CI))	Sens	Spec
Long axis	0.69 (0.54–0.84)		
>8 mm		0.80	0.32
>10 mm		0.73	0.54
>12 mm		0.53	0.82
>14 mm		0.40	0.87
>16 mm		0.20	0.94
Short Axis	0.81 (0.70–0.91)		
>5 mm		0.80	0.57
>6 mm		0.67	0.79
>7 mm		0.47	0.89
>8 mm		0.47	0.95
>9 mm		0.33	0.98
>10 mm		0.27	0.99
Ratio	0.67 (0.54–0.79)		
>0.5		0.80	0.45
>0.6		0.53	0.73
>0.7		0.47	0.77
>0.8		0.27	0.89
>0.9		0.07	0.96
ADC	0.62 (0.48–0.76)		
<0.00080		0.93	0.27
<0.00070		0.71	0.51
<0.00065		0.36	0.74
<0.00060		0.36	0.76
<0.00055		0.29	0.85
<0.00050		0.29	0.93
Border			
Lobulated	0.51 (0.36–0.66)	0.27	0.75
Spiculated	0.49 (0.35–0.64)	0.00	0.98
Indistinct	0.49 (0.34–0.64)	0.00	0.98

diameter combined with ADC were computed for several cut-off values. Best sensitivity and specificity rates are acquired by combined short axis diameter >8 mm with an ADC $< 0.80 \times 10^{-3}$ mm^2/s, resulting in a sensitivity of 42.9 (95% CI 16.9–68.8) ($p = 0.63$ compared to SA > 8 mm alone) and specificity 96.6 (95% CI 94.8–98.3) ($p = 1.0$ respectively). Characterising the border of a lymph node had the worst test performance (AUC = 0.49–0.51) (Table 4).

We performed sensitivity analyses – by excluding the case with IIB disease and the patients with >6 weeks between scan and surgery – however this did not change the results.

4. Discussion

There is a growing awareness of the limited diagnostic accuracy of morphologic imaging criteria for staging lymph nodes even at high and ultra-high field strengths.[11] The ADC of lymph nodes is low, so both benign and metastatic lymph nodes are bright on high *b*-value diffusion-weighted images. This facilitates their recognition and discrimination from vessels and other pelvic structures.[4,5] Using ADC as imaging biomarker is attractive because it is non-invasive, does not require exogenous contrast agents or ionising radiation and is easily incorporated into routine MRI protocols.

A series of patients ($n = 25$) with cervical cancer was preoperatively scanned on a 3 T MR scanner by Yu et al.[12] In this study the ADCs of 17 metastatic pelvic lymph nodes found at histopathological evaluation were compared to the ADCs of 140 benign nodes. A statistical significant difference in ADC was found between normal and metastatic nodes ($0.86 \pm 0.36 \times 10^{-3}$ versus $1.12 \pm 0.34 \times 10^{-3}$ mm^2/s, $p = 0.004$). The diagnostic performance of DWI was not evaluated in this study.

The ADC threshold for discriminating metastatic from benign nodes in cervical cancer patients varied largely studies: 0.712×10^{-3}–1.15×10^{-3} mm^2/s.[6,8] Alternatives were sought, such as using the relative ADC (dividing or subtracting lymph node ADC by tumour ADC), to assess the nodal status with conflicting results.[6,8,13] In our analysis (data not shown) relative ADC between tumour and lymph node or muscle and lymph node was not significantly different in metastatic and normal lymph nodes.

An important alternative competing with functional imaging in cervical cancer staging is the sentinel lymph node biopsy (SNB) in cervical cancer patients. Recently a multi-centre study involving 145 cervical cancer patients showed a sensitivity of 92% and a negative predictive value of 98.2%.[14] There were no false-negative results in 76.5% of the patients in whom the sentinel lymph nodes were detected bilaterally. It must be noticed that all sentinel nodes were evaluated by ultra-staging; a time-consuming method which cannot be performed during surgery. Since the start of our study some clinics started to use SNB staging in early stage cervical cancer patients. However, to date a complete pelvic lymphadenectomy without SNB in early-stage cervical cancer is still advised by international guidelines.[15,16]

A few limitations of our study should be considered. First, a node-by-node analysis could not be performed because it was not feasible to remove and evaluate node bearing tissue in the exact anatomic position in which it is found in the pelvis. Comparison on regional level was considered the best possible estimate we could provide. Also, by mismatching of the number of nodes identified by radiologist and pathologist we decided to match the largest node (measure by radiologist) to be the malignant one. This approach could introduce bias, however by performing a region-by-region comparison results presented are less susceptible to bias. Blinding of the observers to clinical parameters such as age, tumour type and clinical stage is not according to clinical practice, but in an experimental setting it is the best way to avoid bias. Finally, we included a relatively small number of women with only a few positive lymph nodes. Although cervical cancer is the third most common cancer in women with worldwide 530,000 new cases each year,[17] 85% of these patients present in developing coun-

tries with limited resources. It is clear that multi-centre and likely also multinational prospective studies are needed to improve care in cervical cancer patients.

In conclusion, the results of this prospective, dual-centre clinical study demonstrate that the sensitivity of conventional MRI to detect metastatic pelvic lymph nodes in cervical cancer patients is modest. ADC does not improve the diagnostic performance of the best discriminator, short axis diameter, to distinguish malignant from non-malignant pelvic lymph nodes in early stage cervical cancer patients. The clinical relevance of ADC to detect lymphatic metastasis is currently low.

Conflict of interest statement

None declared.

Acknowledgements

The IKL, location Utrecht, had no involvement in study design; in the collection, analysis and interpretation of data; in the writing of the report; and in the decision to submit the paper for publication.

References

1. Quinn MA, Benedet JL, Odicino F, et al. Carcinoma of the cervix uteri Volume 26 of the FIGO annual report on the results of treatment in gynaecological cancer. *Int J Gynaecol Obstet* 2006;**95**(Suppl. 1):S43–103.
2. Bipat S, Glas AS, van der Velden J, et al. Computed tomography and magnetic resonance imaging in staging of uterine cervical carcinoma: a systematic review. *Gynaecol Oncol* 2003;**91**:59–66.
3. Scheidler J, Hricak H, Yu KK, Subak L, Segal MR. Radiological evaluation of lymph node metastases in patients with cervical cancer. A meta-analysis. *JAMA* 1997;**278**:1096–101.
4. Koh DM, Collins DJ. Diffusion-weighted MRI in the body: applications and challenges in oncology. *Am J Roentgenol* 2007;**188**:1622–35.
5. Takahara T, Imai Y, Yamashita T, et al. Diffusion weighted whole body imaging with background body signal suppression (DWIBS): technical improvement using free breathing, STIR and high resolution 3D display. *Radiat Med* 2004;**22**:275–82.
6. Chen YB, Liao J, Xie R, Chen GL, Chen G. Discrimination of metastatic from hyperplastic pelvic lymph nodes in patients with cervical cancer by diffusion-weighted magnetic resonance imaging. *Abdom Imaging* 2011;**36**:102–9.
7. Park SO, Kim JK, Kim KA, et al. Relative apparent diffusion coefficient: determination of reference site and validation of benefit for detecting metastatic lymph nodes in uterine cervical cancer. *J Magn Reson Imaging* 2009;**29**:383–90.
8. Lin G, Ho KC, Wang JJ, et al. Detection of lymph node metastasis in cervical and uterine cancers by diffusion-weighted magnetic resonance imaging at 3T. *J Magn Reson Imaging* 2008;**28**:128–35.
9. Choi EK, Kim JK, Choi HJ, et al. Node-by-node correlation between MR and PET/CT in patients with uterine cervical cancer: diffusion-weighted imaging versus size-based criteria on T2WI. *Eur Radiol* 2009;**19**:2024–32.
10. Mir N, Sohaib SA, Collins D, Koh DM. Fusion of high b-value diffusion-weighted and T2-weighted MR images improves identification of lymph nodes in the pelvis. *J Med Imaging Radiat Oncol* 2010;**54**:358–64.
11. Korteweg M, Zwanenburg JJ, Hoogduin JM, et al. Dissected sentinel lymph nodes of breast cancer patients: characterization with high-spatial-resolution 7-T MR imaging. *Radiology* 2011;**261**:127–35.
12. Yu SP, He L, Liu B, et al. Differential diagnosis of metastasis from non-metastatic lymph nodes in cervical cancers: pilot study of diffusion weighted imaging with background suppression at 3T magnetic resonance. *Chin Med J (Engl)* 2010;**123**:2820–4.
13. Liu Y, Liu H, Bai X, et al. Differentiation of metastatic from non-metastatic lymph nodes in patients with uterine cervical cancer using diffusion-weighted imaging. *Gynaecol Oncol* 2011;**122**:19–24.
14. Lécuru F, Mathevet P, Querleu D, et al. Bilateral negative sentinel nodes accurately predict absence of lymph node metastasis in early cervical cancer: results of the SENTICOL study. *J Clin Oncol* 2011;**29**:1686–91.
15. Haie-Meder C, Morice P, Castiglione M. Cervical cancer: ESMO Clinical Practice Guidelines for diagnosis, treatment and follow-up. *Ann Oncol* 2010;**21**(Suppl. 5):v37–40.
16. National Cancer Institute. Cervical cancer treatment (PDQ®) http://cancer.gov/cancertopics/pdq/treatment/cervical/HealthProfessional.
17. GLOBOCAN 2008, International Agency for Research on Cancer, Section of Cancer Information. IARC, 150 Cours Albert Thomas, 69372 Lyon CEDEX 08, France.